EAI Endorsed Transactions
on Scalable Information Systems
Research Article EAI.EU

Eye Disease Detection Using Deep Learning Models with Transfer Learning Techniques

Kalla Bharath Vardhan[1], Mandava Nidhish[2], Surya Kiran C.[3], Nahid Shameem D.[4], Sai Charan V.[5], R.M. Bhavadharini[6,*]

[1,2,3,4,5,6] School of Computer Science and Engineering, Vellore Institute of Technology, Chennai, India.

Abstract

INTRODUCTION: Diabetic Retinopathy, Cataract and Glaucoma are the major eye diseases posing significant diagnostic challenges due to their asymptotic nature at their early stages. These diseases if not detected and diagnosed at their early stages may lead to severe visual impairment and even can cause blindness in human beings. Early detection of eye diseases showed an exceptional recovery rate. Traditional diagnostic methods primarily relying on expertise in the field of ophthalmology involve a time-consuming process. With technological advancements in the field of imaging techniques, a large volume of medical images have been created which can be utilized for developing more accurate diagnostic tools in the field. Deep learning (DL) models are playing a significant role in analyzing medical images. DL algorithms can automatically learn the features which indicate eye diseases from eye image datasets. Training DL models, however, requires a significant amount of data and computational resources. To overcome this, we use advanced deep learning algorithms combined with transfer-learning techniques. Leveraging the power of deep learning, we aim to develop sophisticated models that can distinguish different eye diseases in medical image data.
OBJECTIVES: To improve the accuracy and efficiency of early detection methods, improve diagnostic precision, and intervene in these challenging ocular conditions in a timely manner.
METHODS: The well-known Deep Learning architectures VGG19, InceptionV3 and ResNet50 architectures with transfer learning were evaluated and the results are compared.
RESULTS: VGG19, InceptionV3 and ResNet50 architectures with transfer learning achieved 90.33%, 89.8% and 99.94% accuracies, respectively. The precision, recall, and F1 scores for VGG19 were recorded as 79.17%, 79.17%, and 78.21%, while InceptionV3 showed 82.56%, 82.38%, and 82.11% and ResNet50 has 96.28%, 96.2%, and 96.24%.
CONCLUSION: The Convolutional Neural Network models VGG19, Inception v3, ResNet50 combined with transfer learning achieve better results than the original Convolutional Neural Network models

Keywords: Deep Learning (DL), Transfer Learning (TL), CNN, VGG19, ResNet50, InceptionV3, Cataract, Diabetic Retinopathy, Glaucoma

Received on 02 03 2024, accepted on 10 06 2024, published on 19 07 2024

doi: 10.4108/eetsis.5971

1. Introduction

Cataract, Glaucoma, and Diabetic Retinopathy (DR) are dangerous eye diseases which cause damage in the optic nerve and everlasting blindness in human beings. Diabetes sufferers frequently exhibit an increased glucose level within the body, which leads to various eye conditions, which include but are not limited to cataracts, diabetic macular edema, DR and glaucoma, amongst others. The International Diabetes Federation (IDF) stated that 1 in 8 adults will have diabetes by the year 2045, which also indicates a susceptibility to having such eye conditions.

*Corresponding author. Email: bhavadharini.rm@vit.ac.in

Cataracts often develop due to factors such as aging and excessive exposure to sunlight when the proteins in the eye lens clump together, hindering light's passage through the lens, resulting in unclear vision. Opacity and cloudiness within the inner lens of the eye are symptoms indicative of cataract disease. The use of fundus pictures for eye disease detection holds a specific importance in providing timely support to patients in underdeveloped areas [1]. An unidentified and untreated cataract in its early stages is the main cause of blindness, with nearly 18 million people losing sight in both eyes [4].

DR is a complication arising from diabetes where prolonged high blood sugar levels in human body causes significant damage to the blood vessels within the retina, leading to vessel leakage [11]. Managing DR requires regular eye examinations, effective blood sugar control, and timely medical intervention. The traditional screening method for identifying DR is time-consuming, necessitating ophthalmologists identifying critical features from structural eye images [13]. DR poses a significant threat to the retina, involving structural changes such as microaneurysms (MAs), exudates (EXs), haemorrhages (HMs), and the development of additional blood vessels [15].

Glaucoma is known as a "silent thief of sight". as it causes increased degeneration of nerve fibres where symptoms cannot be identified until the disease reaches an advanced stage, leading to gradual and irreversible vision loss. [24]. Glaucoma is also an irreversible neurodegenerative disorder, characterized by asymptomatic progression, resulting in sustained vision deterioration due to delayed detection [25].

The utilization of Deep Learning (DL) and Transfer Learning (TL) methods are extensive in the field of eye disease detection. They involve collecting images from diseased and normal eyes, which are then subjected to image pre-processing to minimize interference. The pre-processed images are subsequently fed into a DL architecture, optimizing input data to classify unseen eye datasets. The architecture effectively classifies and labels diseased eyes, providing specific information about the type of eye disease present. The TL approach, which involves utilizing a pre-trained model often trained with vast datasets, enables the adaptation of knowledge from an existing task to a designated task. The TL approach is particularly beneficial when dealing with a limited number of images or aiming to reduce training time. The objective of the proposed work is to enhance the performance of Convolutional Neural Networks (CNN) models, recognizing that the overall effectiveness of the architecture can be influenced by the quality of images in the dataset. This research aims to refine and optimize deep learning methods for the accurate and efficient detection of various eye conditions.

2. Literature Survey

Cataracts come in varied forms - nuclear, cortical, and posterior subcapsular - obstructing the visibility of the retinal structure which necessitates the urgent need for inexpensive diagnostic tools, particularly in rural areas. Macular Pigment (MP) measurement, critical for maintaining visual function, faces numerous challenges in clinical practice due to the complexities involved in assessment. Fundus reflectometry and autofluorescence spectroscopy are potential solutions, albeit with limitations when dealing with elder people facing cataracts. Artificial Intelligence (AI) aided measurement holds great potential in tackling these obstacles, facilitating a precise evaluation of MP for the efficient management of age-related macular degeneration and visual impairments. The entire situation prompts heavy research and development efforts to provide practical solutions for cataract-related issues, emphasizing the critical need for improved detection and treatment strategies in the fight against visual impairments [1,2]. Increasing the depth of CNN architecture is beneficial for classification accuracy [3]. Deep convolutional networks have been evaluated (up to 19 weight layers) for largescale image classification. The residual learning framework was presented in [4] to enhance the performance of very deep neural networks. Authors have also explored ways to scale up networks by maximizing the efficiency of additional computational resources [5]. This was achieved through strategies such as appropriately factorized convolutions and rigorous regularization techniques. One study presents a two-phase strategy [6]: the Deep OCRN_IAO model identifies cataracts using retinal and lamp images, followed by BE_ResNet101 for type and grade classification. With an accuracy of 98.87%, specificity of 99.66%, and sensitivity of 98.28%, the model shows significant enhancements in diagnosing cataracts. Research work has introduced an innovative approach using videos of lens scans from mobile phone slit lamps, enhancing accuracy and efficiency through YOLOv3-based positioning and classification [7]. The proposed algorithm demonstrates promise for real-time cataract grading, improving accessibility to screening services in rural and urban areas. Integrated with mobile slit lamps, it enables community health workers to extend screening services to patients' homes and rural health stations, lessening the burden of undiagnosed cataracts and related illnesses.

Two deep learning models were discussed in aiding cataract diagnosis [8], leveraging a fundus dataset for automatic classification of normal and cataract images. The Mobile Net V3 Small model gives a notable result of 8.26% accuracy improvement over the basic model after fine tuning and layer additions. When tested on these combined datasets, the Mobile Net V3 model achieves an average accuracy of around 96.62%. The proposed DCNN model [9] shows some robust performance, with accuracies of 97% for cataract classification and 98% for non-cataract images. Leveraging retinal fundus images post-G-filter enhances classification accuracy and stability, outperforming many existing methods. This approach holds great promise for real-time cataract detection and diagnosis, offering practical significance in early screening and diagnosis of eye diseases, with maybe some potential for broader application in the field.

Globally, vision impairment affects millions, with cataracts a leading cause, especially in developing regions. By leveraging deep learning, the study enhances non-invasive cataract diagnosis, addressing rural healthcare challenges. Deep convolution networks effectively classify nonlinear fundus image combinations, improving classification accuracy despite limited datasets. Future efforts aim to refine cataract detection through deep learning advancements, enhancing eye healthcare accessibility and outcomes globally [10,11]. A novel, unique, and innovative approach combining the Deep Convolutional Neural Network (DCNN) with Random Forest (RF) is meticulously proposed cataract grading, achieving an excellent average accuracy of 90.69%. This method significantly enhances specificity and sensitivity indicators, enabling a more precise assessment of the patient's condition. This strongly suggests the enormous potential for a more cost-effective and simplified cataract diagnosis process, particularly in underserved regions, efficiently addressing critical healthcare needs with unparalleled accuracy and efficiency [12,13].

DR stands as a significant diabetes complication, causing irreversible damage to retinal blood vessels and potential blindness if left undetected. Early diagnosis is crucial, yet current treatments mainly focus on delaying sight deterioration. Advanced computer-based systems offer promise in early detection, surpassing manual methods and reducing time and cost burdens. DR images are classified into different stages and localization of the lesions on the retinal surface is performed by DL models. The first model, CNN512, achieved an 88.6%, accuracy on DDR and APTOS Kaggle 2019 datasets. Fusion of both models yields 89% accuracy, outperforming current standards. [14,15]. The manual detection of DR is extremely challenging due to its structural impact on the retina, which may cause microaneurysms, exudates, haemorrhages, and abnormal blood vessel growth. The transfer learning approach has been deployed for detecting and classifying DR in fundus images, for the purpose of feature extraction in binary and multiclass classification. The system achieved 97.8% and 89.29% accuracy, with the modified method reaching for binary classification and multiclass classification respectively [16,17]. Artificial Intelligence-based screening systems have become essential requirements for efficiently analysing Retinal Fundus Images (RFI) in less economically developed countries. With this aim, a novel lightweight CNN model was designed particularly for binary classification with a minimal computational cost, achieving notable metrics including 98.6% area under the curve, 97.66% sensitivity, and 98.33% specificity. Additionally, an object detection model was trained to enhance retinal image suitability, achieving a mean average precision of 94.5% [18,19].

CNNs streamline medical image analysis, but training them remains challenging, particularly with predominantly easy-to-classify samples. A faster CNN model was used in training medical images by dynamically selecting misclassified negative samples during training, focusing on haemorrhage detection in fundus images. Integrated selective sampling reduces training time while maintaining high performance. Achieving 94.5% accuracy, CNNs outperform conventional approaches, with the potential for clinical integration to streamline diagnosis; promising to enhance medical image analysis workflows [20,21]. A two-step Deep Convolutional Neural Network (DCNN) algorithm can effectively pinpoint lesion locations and types within fundus images, concurrently providing severity levels of DR. By combining local and global networks, the feature learning process for DR analysis is significantly improved. Moreover, the introduction of an unbalanced weighting map serves to prioritize lesion patches for accurate DR grading, ultimately boosting algorithm performance. [22,23].

The TL model is integrated with the U-Net structure for optic cup segmentation and DenseNet-201 for characteristic extraction. DCNN approach classifies images to ascertain glaucoma presence, aiming to apprehend the situation in retinal fundus images. Performance metrics like accuracy, precision, recall, and the F1 score validate the model’s efficacy, with an accuracy of 98.82% in training and 96.90% testing [24,25]. A DL Polynomial Driven Glaucoma Classification Net (PDGC-Net)-based multi-stage was designed for detecting Glaucoma in fundus images. This model begins with noise estimation and reduction using polynomial coefficients. PDGC-Net made use of polynomial indeterminate blocks designed with CNN architectures for image classification, displaying high accuracy ranges on various fundus image datasets. Model elasticity is tested across PDGC-Net stages, and quantitative analysis against state-of-the-art CNN models affirms its efficacy for glaucoma screening. The study takes heed of the significance of noise estimation and reduction in image preprocessing and proudly showcases PDGC-Net's adaptability across diverse datasets [26,27]. The effectiveness of a profound learning ensemble approach employing ONH enface images from SLO in distinguishing Glaucoma patients from healthy humans was analyzed. The preliminary categorization was dependent on various clinical tests: intraocular pressure measurements, visual fields, Optical Coherence Tomography (OCT)-derived RNFL thickness, and ONH examination. A task-specific CNN structure was formulated for SLO image-based classification, outperforming other tested classifiers, including machine learning methods and RNFL thickness-based ones. SLO images coupled with DL methods show potential in glaucoma diagnosis, especially in cases with limited data. Despite the limited dataset, the DL ensemble accomplished high accuracy, hinting at its potential in supporting glaucoma diagnosis. As people become older, the prevalence of glaucoma rises, demanding efficient diagnostic tools to counteract its impact on individuals and societies. Improved awareness and proactive management strategies are vital in addressing difficulties of glaucoma-related visual impairments and economic costs, improving early identification and treatment to mitigate disease progression [28-31].

Various ImageNet-trained models, including Visual Geometry Group 16 -(VGG16 and VGG19), InceptionV3, Residual Network (ResNet50), and Xception, were explored on fundus images for automatic Glaucoma assessment. Using

five public databases comprising 1707 images, the Xception architecture achieved significant performance improvements, yielding an average Area Under Curve (AUC) of 0.9605, 95% confidence interval of 95.92–97.07%, an average specificity of 0.8580 and sensitivity of 0.9346. ACRIMA, containing 705 labelled images, has been introduced as a new clinical database, the largest public database for glaucoma diagnosis, supporting the high specificity and sensitivity obtained. [32,33].

Recent research studies analyzed varied datasets comprising fundus images that represent four primary eye diseases: Diabetic Retinopathy (DR), Glaucoma, Myopia, and Normal. These works concentrated on automatic detection and analysis of eye diseases, paving the way for future improvements in clinical era and affected person care [34,35]. Authors explored small labelled statistics for 3 eye disorder predictions [36], which are, 1) vast class prediction, 2) satisfactory-grained sickness sub-class prediction, and 3) textual diagnosis technology. Challenges encompass small record length, multi-project predictions, dealing with picture versions, and hyper-parameter choice. Authors explored these challenges inside a multi-task learning (MTL) framework [37] and recommended a singular MTL-primarily based trainer ensemble approach for know-how distillation. On a dataset of 43,066 fundus photos from 3,502 patients, 7,212 photos were categorized and the rest were not labelled. The proposed method achieved around 83% accuracy in Task 1 and had a 75% accuracy in recognizing key features within the top 5 predictions for Task 2, even though only 15% of the available labelled data was used. Robust and various retinal photograph datasets, including the Indian Diabetic Retinopathy Image Dataset (IDRiD), are crucial for the improvement and evaluation of virtual screening packages and associated algorithms, a result of microvascular retinal adjustments brought on by using diabetes, and stand as a leading motive of preventable blindness globally. Similarly, Diabetic Macular Edema (DME) poses significant difficulty related to DR. Deep Learning, encompassing various machine learning techniques, demonstrates superior performance in photograph processing, computer vision, and pattern recognition as compared to traditional strategies [38,39]. Eye diseases, especially Age-Related Macular Degeneration (AMD), and DME pose large threats to vision, especially in older individuals and diabetic patients. Early detection through optical coherence tomography (OCT) imaging is crucial. Various DL models like VGG-16, Mobile Net, ResNet-50, Inception V3, and Xception have been employed for retinal disease classification, attaining up to 96.21% checking out accuracy, assisting speedy analysis and lowering costs for large-scale research. The capabilities of ResNet-50 combined with the Random Forest class, has confirmed a superior overall performance as compared to modern methods with 96% and 75.09% accuracy on Messidor-2 and EyePACS datasets [40,41]. OCT emerges as a pivotal non-invasive diagnostic tool, supplying special cross-sectional images of the retinal layers. With its ability to come across retinal diseases and abnormalities, OCT aids ophthalmologists in timely diagnosis and remedy-making plans. However, the analysis of OCT images is time-consuming for practitioners because of the multiple images generated per patient. Advanced Machine Learning models are utilize to categorize OCT images into 4 main categories: Choroidal Neovascularization (CNV), Diabetic Macular Edema (DME), Drusen, and normal retinas. Using binary CNN classifiers based on well-known models like VGG16, VGG19, ResNet50, ResNet152, DenseNet121, and InceptionV3, the models showed promising results. The best-performing model achieved impressive metrics: 98.7% accuracy, 98.7% sensitivity, and 99.6% specificity. These models could serve as effective secondary tools for ophthalmologists, aiding in the quick and accurate analysis of OCT images. OCT is crucial for providing detailed cross-sectional images of the retina, which are significant for detecting various retinal diseases [42,43].

Precise and timely examination increases the potential for effective treatment of DED and reduces risk of permanent vision loss. A DL approach using a new CNN model has been proposed. This model automates multi-class DED classification from retinal fundus images, tested on publicly available data, and achieved an accuracy of 81.33%, with 100% sensitivity and specificity [44]. Early detection of DED through automated systems using machine learning offers substantial benefits over manual methods, reducing human error and improving efficiency. The survey [45] aims to provide valuable insights for researchers, healthcare professionals, and diabetic patients, highlighting advancements and challenges in automated DED detection. A DL based model has been tested [46]. The top two pretrained CNN models on ImageNet, incorporating fine-tuning, optimization, and contrast enhancement techniques, achieved 88.3% accuracy for multi-class classification, significantly improving diagnostic efficiency and accuracy for ophthalmologists.

Table 1 provides a comparison of different architectures and classifiers for the diagnosis of different diseases such as Glaucoma, DR, Cataract, and combinations of these diseases. Reviews of different architectures such as DenseNet, ResNet, U-Net, CNN and InceptionV3 are evaluated with classifiers such as SVM, Softmax, Random Forest, KNN, etc for each disease group. Hypermetric parameters include Accuracy (Acc), Precision (Pre), Recall (Re), Sensitivity (Sen), Specificity (Sp), F1-score (F1), Area Under the Curve (AUC), and Cohen's Kappa (Ka), where applicable. These results vary across different models and diseases, with some achieving high accuracy and comprehensive performance metrics, while others may show lower accuracy or focus on particular aspects like sensitivity or specificity. Additionally, the table includes cases of mixed diseases, where models are evaluated on a combination of eye disorders.

Table 1. Comparison of results achieved in Literature survey papers

Diseases	Architecture	Authors	Results
Cataract	Dense net	Jayachitra, S., et [1]	Acc=89, Sen=75, Sp=82
	U Net	Jayachitra, S., et [1]	Acc=93.5, Sen=80, Sp=86
	Res Net 101	Saju et al[3]	Acc=98.87, Sen=98.28,Sp=99.66, F1=95.68, Ka=97.83
	ACCV	Hu ey al [4]	Acc=94, Pre=95.8,Sen=92, Sp=96, F1=93.88
	Mobile Net V3s	CETINAR et al [5]	Pre=89, Re=93, F1=90, Acc=89
Diabetic Retinopathy	CNN512, YOLOV3	Alyoubi et al [11]	Acc=89, Sen=89, Sp=97.3, AUC=97
	CNN	Ghan et al [12]	Acc=84, Pre=100, Re=100, F1=100
	Res Net	Bilal et al [14]	Acc=94,Pre=94.15,Sen=93.30, Sp=93.70, F1=93.65,AUC=97
	VGG13	Pinedo-Diaz et al [15]	Acc=99.92, Sen=98.20, Sp=98.33, AUC=98.60
Glaucoma	U-Net, Dense Net-201	Kashyap et al [21]	Acc=98.82, Pre=98.02, Re=97.77, Sp=97.97, F1=97.87
	CNN	Sandoval-Cuellar et al [22]	Acc=93.22, Sen=94.14, AUC=93.98
	PDGC-Net	Naidana et al [23]	Acc=98, Sen=89, Sp=100
	DenseNet161	Schottenhamml et al [24]	Acc=92.3
	InceptionV3	Sulot et al [25]	Acc=96.2
Mixed Diseases	CNN	Smaida et al [31]	Acc=92.1
	Res Net 50		Acc=99.99
	Res Net-18		Acc=61
	Inception V3		Acc=77.5
	Alex Net, Res Net, VGG Net	Nazir et al [32]	Acc=95,75, Sen=94.75, Sp=94.90, AUC=97.85
	VGG 19	Chelaraim Ani et al [33]	Acc=97.33
	Inception V3		Acc =94.86
	Res Net		Acc=98.11
	VGG 16	ElSharif et al [37]	Acc=92.95,Pre=93.50,Sen=93.20, Sp=92.70,F1=93.50,AUC=93.56, Ka=86.94
	Inception V3	ElSharif et al [37]	Acc=91.03,Pre=91,Sen=91.16, Sp=90.91,F1=91,AUC=91.31, Ka=82.55

3. Materials and Methods

The proposed work assesses the well-known CNN architectures VGG-19, Inception V3, ResNet50 and the same CNN models are evaluated using TL approach with the weights learnt from ImageNet dataset. Proposed models are evaluated using publicly accessible dataset that includes fundus images covering eye diseases such as cataract, diabetic retinopathy, glaucoma, and normal eye conditions.

3.1. Dataset Description

The dataset "eye_diseases_classification (Eye Disease Retinal Images)" from Kaggle is taken for evaluating the models. This dataset comprises approximately 1000 retinal images for each class: Normal, DR (Diabetic Retinopathy), Cataract, and Glaucoma. These images are gathered from diverse sources such as IDRiD, Ocular Recognition, HRF, among others. Table 2 shows the number of images in each eye disease class in dataset.

Table 2: Dataset Description

S.No.	Types of Diseases	Total images	Training images	Testing images
1.	Cataract	1038	830	208
2.	Diabetic Retinopathy	1098	878	220
3.	Glaucoma	1007	806	201
4.	Normal	1074	859	215

3.2. VGG 19

VGG 19 is a CNN architecture widely used in image classification and renowned for its simplicity and effectiveness in classification tasks. VGG 19, as shown in Fig.1, has a total of 19 layers consisting of 16 convolution layers followed by 3 fully connected layers. Each convolutional layer uses a 3x3 filter, with a stride of one

and padding to preserve spatial information. The convolutional layers are stacked with rectified linear unit (ReLU) activations, accompanied with max pooling layers to reduce spatial dimensions. After every two convolution layers, spatial dimensions are reduced using Max pooling with a 2x2 window and stride of 2. The fully connected layers have 4,096 units and are followed by a SoftMax layer for categorization.

Convolutional Layer Operation

- For a given layer l, the operation of a convolutional layer in VGG19 can be represented as shown in Equation 1:

$$Y_{i,j,k}^{(l)} = \sigma\left(\sum_{m,n} W_{m,n,k}^{(l)} . X_{i+m,j+n}^{(l-1)} + b_k^{(l)}\right) \quad (1)$$

- $Y_{i,j,k}^{(l)}$ rerpresents the activation on the k-th feature map at position (i, j) in layer l.
- $W^{(l)}$ denotes the weights, $X^{(l-1)}$ represents the activations from the previous layer, and $b^{(l)}$is the bias term.
- σ denotes the activation function, typically ReLU.

ReLU Activation

- Applied element-wise, the ReLU activation function can be represented as shown in Equation 2.

$$ReLU(x) = max(0, x) \quad (2)$$

Fully Connected Layer

- The output from the convolutional layers is flattened and passed into fully connected layers.
- If W is the weight matrix and b is the bias vector, the function can be represented as shown in Equation 3.

$$y = W \cdot x + b \quad (3)$$

Max Pooling Operation

- Max-pooling in VGG19 can be represented as shown in Equation 4.

$$Y_{i,j,k}^{(l)} = max_{m,n \in R_s} X_{i+m,j+n}^{(l-1)} \quad (4)$$

- R_s denotes the receptive field size

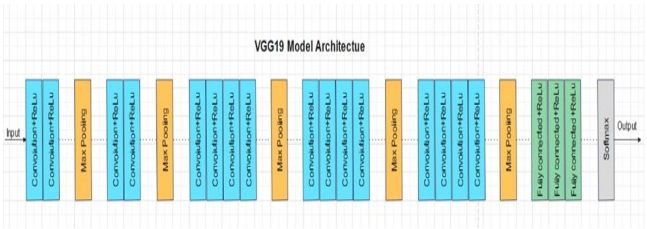

Figure 1. VGG19 Model Architecture

3.3. VGG19 with Transfer Learning

As shown in Fig.2, in VGG19 architecture with TL approach, the top layer of VGG19 has been eliminated, and new layers inclusive of a dense layer, batch normalization, and a flattened layer are integrated.

Dense Layer:

This is a fully connected layer that facilitates the model to learn complex relationships between features extracted from convolutional layers. Each neuron in this layer is connected to every other neuron in the preceding layer, allowing the model to capture intricate patterns and dependencies within the data. By learning these patterns, the model is highly adaptable to a wide range of tasks, from image classification to regression and beyond. Equation 5 denotes the function of Dense Layer.

$$Z = Wx + b \quad (5)$$

Where, Z denotes output vector, W is the weight matrix, x is the input vector, and b is the bias vector.

Batch Normalization:

Batch Normalization helps in stabilizing and accelerating the training process by standardizing the inputs to a layer for each mini-batch. This allows the network to reach higher learning rates and reduces the number of epochs required, making the training smoother and faster. Batch normalization is a form of regularization, reducing the need for other regularization techniques such as dropout. It normalizes the input to each layer to have mean 0 and variance 1 and given by Equation 6.

$$\hat{x} = \frac{x - \mu}{\sqrt{\sigma^2 + \epsilon}} \quad (6)$$

• Where μ and σ^2 are the mean and variance of the batch, and ϵ is a small constant.

Flattening layer

This layer bridges the gap between convolutional feature extraction and dense layer processing by transforming multidimensional output from the convolutional layer into a one-dimensional input. This effectively creates a feature vector that summarizes the most salient aspects of the data, ready for the final classification or regression tasks, and checks for correct data format for further learning.

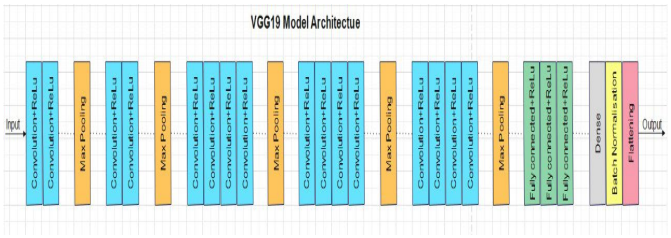

Figure 2. Modified VGG19 Model Architecture

3.4 ResNet50

ResNet50, short for Residual Network with 50 layers, represents a complex architecture in deep learning as shown in Fig.3. Developed by Microsoft Research, ResNet50 stands for its inventive use of residual connections, which deal with the vanishing gradient problem faced during training of Deep Neural Networks. This architecture consists of 50 layers, along with convolutional layers, pooling layers, and fully connected layers. Its residual blocks are an important part of this architecture, wherein shortcut connections allow gradients to go with the flow more directly during training. This architecture enables the development of deeper networks while retaining practicable complexity and avoiding degradation in accuracy. ResNet50 has validated at ahigh level in diverse applications including object recognition, object detection, and photo segmentation. The capacity to extract complex features from images have made ResNet50 a significant model for deep learning networks.

Residual Block Operation

• The key operation in ResNet50 is the residual block, given by Equation 7.

$$Y^{(l)} = F\left(X^{(l)}, \left\{W_i^{(l)}\right\}\right) + X^{(l)} \quad (7)$$

- F represents a series of convolutional layers with batch normalization and ReLU activation functions.
- W_i^((l)) represents the learnable parameters of the residual block in layer l.

Identity Shortcut

• When the input and output dimensions are the same given Equation 8.

$$y = F(x, \{Wi\}) + x \quad (8)$$

Projection Shortcut

• When the input and output dimensions differ, a linear projection Ws is used as shown in Equation 9:

$$y = F(x, \{Wi\}) + Wsx \quad (9)$$

Bottleneck Architecture

• Uses a stack of 1x1, 3x3, and 1x1 convolutions to reduce computation as shown in Equation 10:

$$y = W1(W2(W3x)) \quad (10)$$

• Where $W1$ is the 1x1 convolution reducing dimensions, $W2$ is the 3x3 convolution, and $W3$ is the 1x1 convolution restoring dimensions.

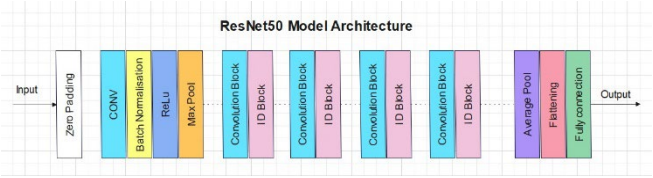

Figure 3. ResNet50 Model Architecture

3.5 ResNet50 with Transfer Learning

As shown in Fig 4, in this modified version of the ResNet50 architecture, the top layer is replaced with additional layers. Two layers of batch normalization, a Dense- ReLU layer and a Dense-SoftMax layer are added. The new layers are:

Batch Normalization Layers

This layer can lead to faster convergence during training, by reducing internal covariate shift and allows each layer of the network to learn more independently of the others. It normalizes the activations of each layer to make training more stable and faster.

Dense-ReLU Layer

The dense layer helps the network understand complex relationships in the data by providing more parameters and flexibility in learning features. The non-linearity through ReLU activations allows the network to model more complex patterns and relationships existing in the data, enabling the network to learn and represent more intricate features. Equation 11 shows the output obtained by combining the Dense layer with ReLU activation function.

$$a = ReLU(z) = \max(0, z) \quad (11)$$

Where z is the output from the Dense layer as defined in VGG19.

Dense-SoftMax layer

Similar to the previous dense layer, this layer also captures more complex relationships in the data, transforming and combining features learned from previous layers into the final output. Also, the SoftMax layer ensures that the network outputs a probability distribution across possible classes, facilitating decision-making based on the highest probability class.

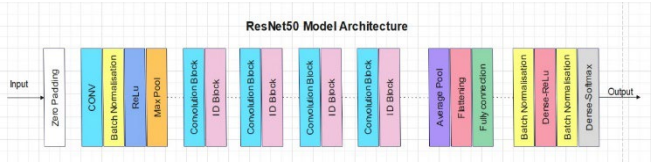

Figure 4. Modified ResNet50 Model Architecture

3.6 InceptionV3

InceptionV3 as shown in Fig.5 represents a significant development in Convolutional Neural Network (CNN) architectures, especially designed for image classification and recognition tasks. Developed by Google researchers, InceptionV3 is renowned for its innovative use of inception modules, which permit the network to seize and technique features at more than one spatial scale. This model has a complex structure that includes various kernel sizes, permitting the model to extract coarse-grained features from input images. Furthermore, the structure employs auxiliary classifiers at some stage in training to mitigate the vanishing gradient problem. Its versatility, performance, and superior overall performance have made InceptionV3 of significant imporance within the field of gaining deep knowledge for computer vision.

Inception Module Operation

- The operation of an inception module in inceptionV3 involves concatenating feature maps obtained from different convolutional filters as shown in Equation 12.

$$Y^{(l)} = concat(Conv1x1, Conv3x3, Conv5x5, MaxPool) \quad (12)$$

- Here, $Y^{(l)}$ represents the output feature map
- Concat denotes the concatenation operation

Auxiliary Classifier Operation

- In InceptionV3, auxiliary classifiers are added to combat the vanishing gradient problem and is given as shown by Equation 13.

$$Y^{(l)} = \sigma(W^{(l)}X^{(l)} + b^{(l)} \quad (13)$$

- $W^{(l)}$and $b^{(l)}$ represent weights and biases of the auxiliary classifier.

Batch Normalization

• Normalizes the input to each layer to have mean 0 and variance 1 and given by Equation 14.

$$\hat{x} = \frac{x - \mu}{\sqrt{\sigma^2 + \epsilon}} \quad (14)$$

• Where μ and σ^2 are the mean and variance of the batch, and ϵ is a small constant.

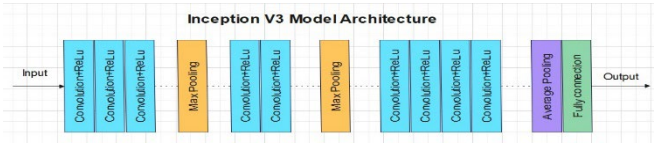

Figure 5. Inception V3 Model Architecture

3.7 InceptionV3 with Transfer Learning

As shown in Fig.6, in modified InceptionV3 architecture, the top layer has been removed to facilitate adjustments that enhance its functionality and adaptableness for specific requirements. The inclusion of a flattened layer serves to reshape the output of the previous layers right into a one-dimensional array, preparing it to get into the next layers. Additionally, the adding of batch normalization layers allows the stabilization and acceleration of the training system via normalizing the input of every layer, which aids in mitigating problems including inner covariate shift and gradient vanishing or exploding. Furthermore, a dense layer has been introduced to permit the connections to learn difficult relationships and styles inside the function space, thereby improving its capability for classification or regression problems.

Our modified version of InceptionV3 has 3 new layers added to the original model and has removed the top layer. These new layers are,

Top layer removal:

Removing the top layer allows flexibility in adapting the network to different tasks or datasets. It simplifies the architecture, making it easier to adjust and fine-tune for specific needs without being constrained by a fixed output layer.

Flattening Layer:

This reshapes the output of previous convolutional and pooling layers into a one-dimensional array. It leverages the hierarchical features learned by convolutional layers for more abstract representations in dense layers.

Batch Normalization Layers:

This layer improves the stability during training by reducing the internal covariate shift and allows for faster convergence. It normalizes the input of each layer by adjusting and scaling activations.

Dense Layer:

This layer allows the network to model more complex decision boundaries and leads to improved accuracy on a challenging basis. It introduces more parameters and non-linearity to the network.

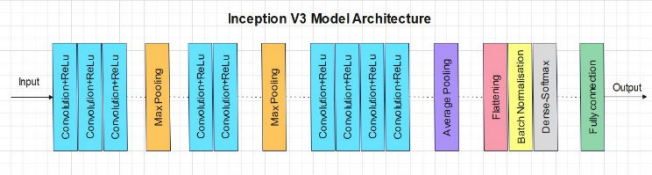

Figure 6. Modified InceptionV3 Model Architecture

4. Results & Discussion

The models VGG-19, ResNet-50 and Inception V3 were evaluated with the dataset and the models have achieved the results depicted in Table 3. A comprehensive overview of training loss, training accuracy, validation loss, and validation accuracy for each model is shown. InceptionV3 recorded the lowest accuracy score of 0.5757 with the highest loss score of 0.9734 and ResNet50 has the highest accuracy score of 0.9534 with the lowest loss score of 0.1320.

Table 3. Performance comparison of VGG-19, ResNet-50 and Inception v3

Model	Loss	Accuracy	Validation loss	Validation accuracy
VGG19	0.6430	0.7384	0.8139	0.6639
ResNet50	0.1320	0.9534	2.6862	0.6550
InceptionV3	0.9734	0.5757	0.9508	0.5704

The modified models under consideration were implemented with varying numbers of epochs: 10 for InceptionV3, 20 for VGG19, and 50 for ResNet50. Following implementation, ResNet50 exhibited the highest accuracy at 0.9994 with an impressively low loss of 0.0023. Table 4 provides detailed information on the training and validation loss, with training and validation accuracy data for each model.

These metrics are essential for evaluating how well the models perform during training and their ability to generalize to new, unseen data. In terms of performance, InceptionV3 recorded the lowest accuracy at 0.898 and the highest loss at 0.2668, coupled with a validation loss of 0.4303 and a validation accuracy of 0.8379. In contrast, ResNet50 demonstrated superior results with the highest accuracy of 0.9994, the lowest loss at 0.0023, a validation loss of 0.2995, and a validation accuracy of 0.9256.

Table 4: Performance of VGG-19, ResNet-50 and Inception v3 models with TL approach.

Model	Loss	Accuracy	Validation loss	Validation accuracy
VGG19	0.2514	0.9033	0.3519	0.8769
ResNet50	0.0023	0.9994	0.2995	0.9256
InceptioV3	0.2668	0.898	0.4303	0.8379

The achieved results of Table 3 and Table 4 have a significant difference, with increase in each model's accuracy also decreasing loss. From this we can state that the modified models showed better performance than the original models.

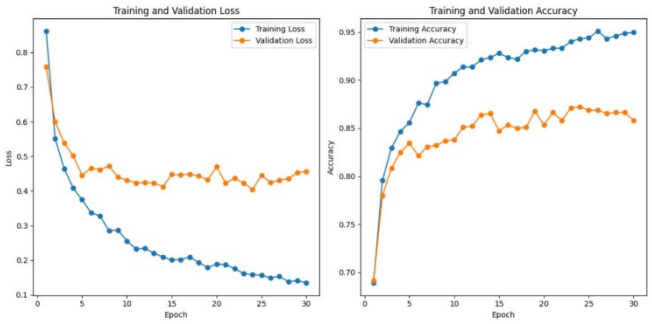

Figure 7. Loss and Accuracy during training and validation phases of Modified Inception V3

Fig.7 shows a positive trend where the epochs progress, with both training and validation loss decrease, while training and validation accuracy increase. This shows that Inception V3 with TL approach is performing effectively, achieving an impressive accuracy of 0.898 with a loss less than 0.3 and validation accuracy of 0.8379 and validation loss of 0.4303.

Figure 8. Loss and Accuracy during training and validation phases of modified VGG19

Fig.8 shows how training loss decreases and accuracy increases with number of epochs. This indicates that VGG19 with a TL approach performs effectively, with an accuracy of 0.9033 an loss less than 0.3 and validation accuracy of 0.8769 and validation loss of 0.3519.

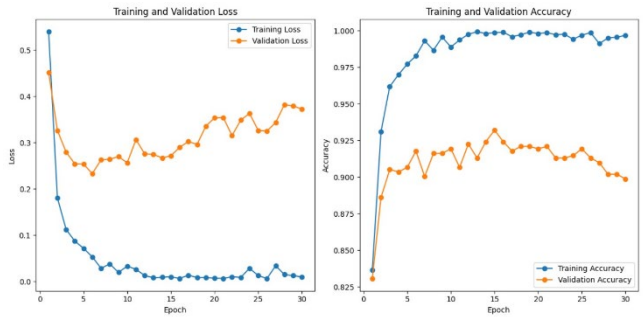

Figure 9. Loss and Accuracy during training and validation phases of modified ReNet50

Fig.9 provides a promising pattern where training and validation loss decrease while training and validation accuracy increase as the number of epochs progress. This shows that ResNet50 with a TL approach is demonstrating good performance, attaining an accuracy of 0.9994 with minimal loss, alongside a validation accuracy of 0.9256 and validation loss of 0.2995. Given its higher accuracy, modified ResNet50 emerges as the preferable model when compared to modified InceptionV3 and modified VGG19.

Table 5: Resulting Hyperparameters

Model	Precision	Recall	F1-score	ROC-AUC
VGG19	79.17	79.17	78.21	49.84
ResNet50	96.28	96.2	96.24	49.60
InceptioV3	82.56	82.38	82.11	51.29

Table 5 compares the performance of three computer vision models—VGG19, ResNet50, and InceptionV3 with a Transfer Learning approach across key metrics. ResNet50 stands out with the highest precision, recall, and F1 score, indicating its superior ability to correctly classify positive instances. However, Inception leads in ROC-AUC, showcasing a better overall classification performance. Modified VGG19 demonstrates competitive precision and recall but lags in F1 score and ROC-AUC. In summary, Modified ResNet50 excels in precision and recall, Modified Inception V3 performs well in overall classification, while Modified VGG19 falls slightly behind in certain metrics. The choice of the ideal model may depend on specific task requirements and the importance of precision, recall, and discriminative ability. Our modified architectural models, including ResNet50, VGG19, and InceptionV3, are designed to work effectively with the Ocular Disease Intelligent Recognition (ODIR) dataset, aiming to achieve maximum accuracy in diagnosing three specific eye diseases: cataract, diabetic retinopathy, and glaucoma. These models have been tailored to handle the complexities and variations within this dataset, ensuring robust performance and high accuracy. The enhancements made to these models not only optimize their performance for the ODIR dataset but also get enhanced well to other eye disease datasets. By incorporating advanced techniques such as data augmentation, dropout for regularization, and fine-tuning of pre-trained models, these models can adapt to different types of ocular images and disease patterns.

4.1 Confusion Matrix:

The confusion matrix indicates true positive and negative and false positive and negative predictions from the proposed model. This defines a model's performance.

True Positives (TP): These are times that the proposed model is correctly recognized as belonging to a selected class.

True Negatives (TN): These are the times that proposed model predicted negative cases correctly. In multi-magnificence class, TN is not generally used due to its extra applicability in binary category settings.

False Positives (FP): These are times that the proposed model incorrectly labelled as belonging to a particular case.

False Negatives (FN): These are instances that the proposed model is incorrectly labelled as not belonging to a specific magnificence.

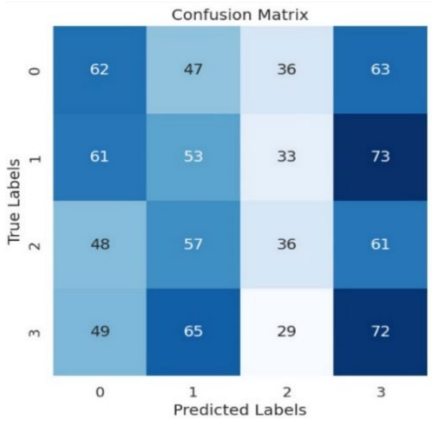

Figure 10. Confusion Matrix for modified VGG19

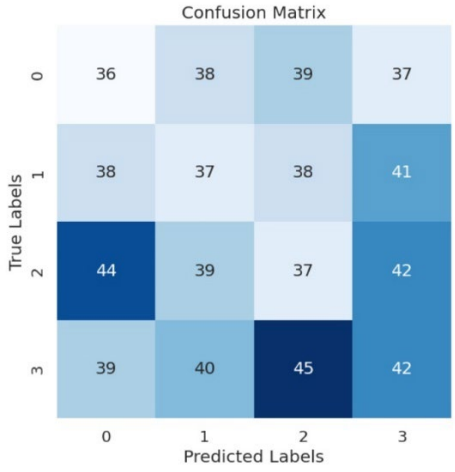

Figure 11a. Confusion Matrix for modified ResNet50

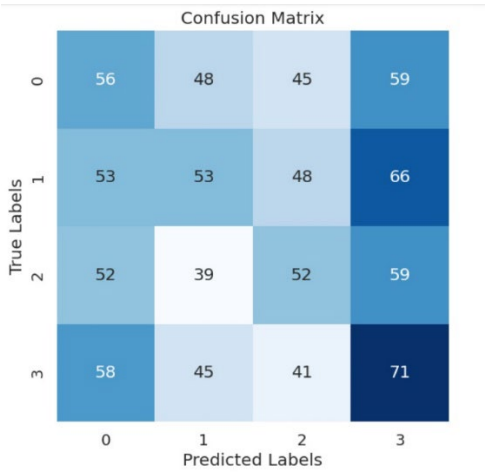

Figure 12. Confusion Matrix for modified InceptionV3

In Fig.10, the confusion matrix works as a comprehensive tool for assessing the model's performance, showcasing the count of true positive, true negative, false positive, and false negative predictions made by VGG19. It shows that for class-0: TP-62, TN-470, FP-146, FN-158 and for class-1: TP-53, TN-384, FP-121, FN-169, and for class-2: TP-36, TN-473, FP-179, FN-153, and for class-3: TP-72, TN-397, FP-116, FN-98. This helps us to understand the errors made by the VGG19 model.

In Fig.11, the confusion matrix works as a comprehensive tool for assessing the model's performance, showcasing the count of true positive, true negative, false positive, and false negative predictions made by ResNet50. It shows that for class-0: TP-36, TN-365, FP-118, FN-113 and for class-1: TP-37, TN-358, FP-119, FN-117, and for class-2: TP-37, TN-354, FP-129, FN-125, and for class-3: TP-42, TN-347, FP-120, FN-129. This helps us to understand the errors made by the ResNet50 model.

In Fig.12, the confusion matrix works as a comprehensive tool for assessing the model's performance, showcasing the count of true positive, true negative, false positive, and false negative predictions made by InceptionV3. It shows that for class-0: TP-56, TN-463, FP-152, FN-163 and for class-1: TP-53, TN-422, FP-138, FN-132, and for class-2: TP-52, TN-438, FP-137, FN-134, and for class-3: TP-71, TN-394, FP-145, FN-145. This helps us to understand the errors made by the InceptionV3 model.

5. Conclusion

The study examined in detail the current status of methods for the detection of Diabetic Eye Disease (DED). After implementing models, we achieved a maximum accuracy of 99% in eye disease detection. The selected datasets were analysed from three aspects: 1) Datasets used, 2) Image preprocessing techniques applied, and 3) Classification methods used. The application of Convolutional Neural Networks (CNNs) and Transfer Learning in analysing eye images has shown promising results, outperforming traditional methods in terms of accuracy and efficiency. In our model Modified ResNet50 achieved a higher accuracy of 0.99, specifically 99.94%. CNN architectures with transfer learning have achieved an accuracy with more precision than the original models. In the referenced research papers, the reported accuracies underscored the efficiency of various models with transfer learning in the given task. The original models of VGG19, ResNet50, InceptionV3 recorded 73.84%, 95.34% and 57.77% accuracies respectively. However, the proposed model, leveraging transfer learning, outperforms the referenced benchmarks, surpassing the reported accuracies with 90.33% for VGG19, 99.94 for ResNet50 and 89.80% for InceptionV3. This achievement positions the proposed model as more efficient for future applications, highlighting its enhanced performance and potential for further advancements in the field.

References

[1] Jayachitra S, Kanna KN, Pavithra G, Ranjeetha T. A novel eye cataract diagnosis and classification using deep neural network. In Journal of Physics: Conference Series 2021 Jun 1 (Vol. 1937, No. 1, p. 012053). IOP Publishing.

[2] Obana A, Ote K, Hashimoto F, Asaoka R, Gohto Y, Okazaki S, Yamada H. Correction for the influence of cataract on macular pigment measurement by autofluorescence technique using deep learning. Translational vision science & technology. 2021 Feb 5;10(2):18-18.

[3] Simonyan, K., & Zisserman, A, Very Deep Convolutional Networks for Large-Scale Image Recognition. *CoRR, abs/1409.1556*, 2014.

[4] He K, Zhang X, Ren S, Sun J. Deep residual learning for image recognition. In Proceedings of the IEEE conference on computer vision and pattern recognition, pp. 770-778,2016.

[5] Szegedy C, Vanhoucke V, Ioffe S, Shlens J, Wojna Z. Rethinking the inception architecture for computer vision. InProceedings of the IEEE conference on computer vision and pattern recognition, pp. 2818-2826, 2016.

[6] Saju B, Rajesh R. Eye-Vision Net: Cataract Detection and Classification in Retinal and Slit Lamp Images using Deep Network. International Journal of Advanced Computer Science and Applications. 2022;13(12).

[7] Hu S, Luan X, Wu H, Wang X, Yan C, Wang J, Liu G, He W. ACCV: automatic classification algorithm of cataract video based on deep learning. BioMedical Engineering OnLine. 2021 Dec; 20:1-7.

[8] ÇETİNER H. Cataract disease classification from fundus images with transfer learning based deep learning model on two ocular disease datasets. Gümüşhane Üniversitesi Fen Bilimleri Dergisi. 2023 Jan;13(2):258-69.

[9] Zhang L, Li J, Han H, Liu B, Yang J, Wang Q. Automatic cataract detection and grading using deep convolutional neural network. In2017 IEEE 14th international conference on networking, sensing and control (ICNSC) 2017 May 16 (pp. 60-65).

[10] Pratap T, Kokil P. Computer-aided diagnosis of cataract using deep transfer learning. Biomedical Signal Processing and Control. 2019 Aug 1;53:101533.

[11] Dong Y, Zhang Q, Qiao Z, Yang JJ. Classification of cataract fundus image based on deep learning. In 2017 IEEE international conference on imaging systems and techniques (IST) 2017 Oct 18 (pp. 1-5).
[12] Ran J, Niu K, He Z, Zhang H, Song H. Cataract detection and grading based on combination of deep convolutional neural network and random forests. In 2018 IEEE international conference on network infrastructure and digital content (IC-NIDC) 2018 Aug 22 (pp. 155-159).
[13] Elloumi Y. Mobile aided system of deep-learning based cataract grading from fundus images. InArtificial Intelligence in Medicine: 19th International Conference on Artificial Intelligence in Medicine, AIME 2021, Virtual Event, June 15–18, 2021, Proceedings 2021 (pp. 355-360). Springer International Publishing.
[14] Alyoubi WL, Abulkhair MF, Shalash WM. Diabetic retinopathy fundus image classification and lesions localization system using deep learning. Sensors. 2021 May 26;21(11):3704.
[15] Ghan G, Chavan S, Chaudhari A. Diabetic retinopathy classification using deep learning. In2020 Fourth International Conference on Inventive Systems and Control (ICISC) 2020 Jan 8 (pp. 761-765).
[16] Butt MM, Iskandar DA, Abdelhamid SE, Latif G, Alghazo R. Diabetic retinopathy detection from fundus images of the eye using hybrid deep learning features. Diagnostics. 2022 Jul 1;12(7):1607.
[17] Bilal A, Zhu L, Deng A, Lu H, Wu N. AI-based automatic detection and classification of diabetic retinopathy using U-Net and deep learning. Symmetry. 2022 Jul 12;14(7):1427.
[18] Pinedo-Diaz G, Ortega-Cisneros S, Moya-Sanchez EU, Rivera J, Mejia-Alvarez P, Rodriguez-Navarrete FJ, Sanchez A. Suitability classification of retinal fundus images for diabetic retinopathy using deep learning. Electronics. 2022 Aug 17;11(16):2564.
[19] Li X, Pang T, Xiong B, Liu W, Liang P, Wang T. Convolutional neural networks based transfer learning for diabetic retinopathy fundus image classification. In2017 10th international congress on image and signal processing, biomedical engineering and informatics (CISP-BMEI) 2017 Oct 14 (pp. 1-11). IEEE.
[20] Sahlsten J, Jaskari J, Kivinen J, Turunen L, Jaanio E, Hietala K, Kaski K. Deep learning fundus image analysis for diabetic retinopathy and macular edema grading. Scientific reports. 2019 Jul 24;9(1):10750.
[21] Xu K, Feng D, Mi H. Deep convolutional neural network-based early automated detection of diabetic retinopathy using fundus image. Molecules. 2017 Nov 23;22(12):2054.
[22] Yang Y, Li T, Li W, Wu H, Fan W, Zhang W. Lesion detection and grading of diabetic retinopathy via two-stages deep convolutional neural networks. In Medical Image Computing and Computer Assisted Intervention− MICCAI 2017: 20th International Conference, Quebec City, QC, Canada, September 11-13, 2017, Proceedings, Part III 20 2017 (pp. 533-540). Springer International Publishing.
[23] Pires R, Avila S, Wainer J, Valle E, Abramoff MD, Rocha A. A data-driven approach to referable diabetic retinopathy detection. Artificial intelligence in medicine. 2019 May 1;96:93-106.
[24] Kashyap R, Nair R, Gangadharan SM, Botto-Tobar M, Farooq S, Rizwan A. Glaucoma detection and classification using improved U-Net Deep Learning Model. InHealthcare 2022 Dec 9 (Vol. 10, No. 12, p. 2497). MDPI.
[25] Sandoval-Cuellar HJ, Alfonso-Francia G, Vázquez-Membrillo MA, Ramos-Arreguín JM, Tovar-Arriaga S. Image-based glaucoma classification using fundus images and deep learning. Revista mexicana de ingeniería biomédica. 2021 Dec;42(3).
[26] Naidana KS, Barpanda SS. Glaucoma classification using a polynomial-driven deep learning approach. Bulletin of Electrical Engineering and Informatics. 2023 Aug 1;12(4):2245-61.
[27] Schottenhamml J, Würfl T, Mardin S, Ploner SB, Husvogt L, Hohberger B, Lämmer R, Mardin C, Maier A. Glaucoma classification in 3 x 3 mm en face macular scans using deep learning in different plexus. Biomedical optics express. 2021 Dec 1;12(12):7434-44.
[28] Sułot D, Alonso-Caneiro D, Ksieniewicz P, Krzyzanowska-Berkowska P, Iskander DR. Glaucoma classification based on scanning laser ophthalmoscopic images using a deep learning ensemble method. Plos one. 2021 Jun 4;16(6):e0252339.
[29] Hemanth DJ, Deperlioglu O, Kose U. An enhanced diabetic retinopathy detection and classification approach using deep convolutional neural network. Neural Computing and Applications. 2020 Feb;32(3):707-21.
[30] Phan, S., Satoh, S.I., Yoda, Y., Kashiwagi, K. and Oshika, T., 2019. Evaluation of deep convolutional neural networks for glaucoma detection. Japanese journal of ophthalmology, 63, pp.276-283.
[31] An G, Omodaka K, Hashimoto K, Tsuda S, Shiga Y, Takada N, Kikawa T, Yokota H, Akiba M, Nakazawa T. Glaucoma diagnosis with machine learning based on optical coherence tomography and color fundus images. Journal of healthcare engineering. 2019;2019(1):4061313.
[32] Diaz-Pinto A, Morales S, Naranjo V, Köhler T, Mossi JM, Navea A. CNNs for automatic glaucoma assessment using fundus images: an extensive validation. Biomedical engineering online. 2019 Dec;18:1-9.
[33] Pal A, Moorthy MR, Shahina A. G-eyenet: A convolutional autoencoding classifier framework for the detection of glaucoma from retinal fundus images. In2018 25th IEEE international conference on image processing (ICIP) 2018 Oct 7 (pp. 2775-2779).
[34] Smaida M, Serhii Y. Comparative Study of Image Classification Algorithms for Eyes Diseases Diagnostic. International Journal of Innovative Science and Research Technology. 2019 Dec;4(12).
[35] Nazir T, Nawaz M, Rashid J, Mahum R, Masood M, Mehmood A, Ali F, Kim J, Kwon HY, Hussain A. Detection of diabetic eye disease from retinal images using a deep learning based CenterNet model. Sensors. 2021 Aug 5;21(16):5283.
[36] Chelaramani S, Gupta M, Agarwal V, Gupta P, Habash R. Multi-task knowledge distillation for eye disease prediction. InProceedings of the IEEE/CVF Winter Conference on Applications of Computer Vision 2021 (pp. 3983-3993).
[37] Sarki R, Ahmed K, Wang H, Zhang Y, Ma J, Wang K. Image preprocessing in classification and identification of diabetic eye diseases. Data Science and Engineering. 2021 Dec;6(4):455-71.
[38] Tan M, Le Q. Efficientnet: Rethinking model scaling for convolutional neural networks. In International conference on machine learning 2019 May 24 (pp. 6105-6114). PMLR.
[39] Krishna ST, Kalluri HK. Deep learning and transfer learning approaches for image classification. International Journal of Recent Technology and Engineering (IJRTE). 2019 Feb;7(5S4):427-32.
[40] Elsharif, A. A. E. F., Abu-Naser, S. S, Retina Diseases Diagnosis Using Deep Learning, International Journal of Academic Engineering Research, Vol.6, Issue. 2, 2022. DOI:10.33022/ijcs.v13i1.3731

[41] Yaqoob MK, Ali SF, Bilal M, Hanif MS, Al-Saggaf UM. ResNet based deep features and random forest classifier for diabetic retinopathy detection. Sensors. 2021 Jun 4;21(11):3883.
[42] Kim J, Tran L. Retinal disease classification from oct images using deep learning algorithms. In2021 IEEE Conference on Computational Intelligence in Bioinformatics and Computational Biology (CIBCB) 2021 Oct 13 (pp. 1-6). IEEE.
[43] Choi JY, Yoo TK, Seo JG, Kwak J, Um TT, Rim TH. Multi-categorical deep learning neural network to classify retinal images: A pilot study employing small database. PloS one. 2017 Nov 2;12(11):e0187336.
[44] Sarki R, Ahmed K, Wang H, Zhang Y, Wang K. Convolutional neural network for multi-class classification of diabetic eye disease. EAI Endorsed Transactions on Scalable Information Systems. 2021 Dec 16;9(4).
[45] Sarki R, Ahmed K, Wang H, Zhang Y. Automated detection of mild and multi-class diabetic eye diseases using deep learning. Health Information Science and Systems. 2020 Oct 8;8(1):32.
[46] Sarki R, Ahmed K, Wang H, Zhang Y. Automatic detection of diabetic eye disease through deep learning using fundus images: a survey. IEEE access. 2020 Aug 10;8:151133-49.